Annual Research & Review in Biology
4(24): 4259-4272, 2014

SCIENCEDOMAIN *international*
www.sciencedomain.org

ECG Generation Based on Action Potential Using Modified Van Der Pol Equation

Mahdi Rezaei Estakhroueieh[1], Seyyed Kamaleddin Yadavar Nikravesh[1*] and Shahriar Gharibzadeh[2]

[1]Department of Electrical Engineering, Amirkabir University of Technology, Tehran, Iran.
[2]Department of Biomedical Engineering, Amirkabir University of Technology, Tehran, Iran.

Authors' contributions

This work was carried out in collaboration between all authors. Author MRE designed the study, proposed the enhanced CEA model, managed the mathematical modeling of the heart, carried out the simulation, compared the results with real data, and wrote the draft of the manuscript. Author SKYN closely supervised the mathematical part of the research. Author SG managed the physiological part of the study. All authors read and approved the final manuscript.

Original Research Article

Received 9th June 2014
Accepted 24th July 2014
Published 3rd August 2014

ABSTRACT

Aims: The aim of this paper is to propose a mathematical model of the cardiac electrical activity in accordance with heart physiology and utilizing this model to generate ECG (electrocardiogram) signal.
Study Design: Modeling the cardiac electrical activity based on physiology of the heart.
Place and Duration of Study: The paper reports the result of a year research in Department of Electrical Engineering, Amirkabir University of Technology, Tehran, Iran.
Methodology: In order to model the cardiac electrical activity, cardiac cells are divided into six parts whose action potentials are modeled by modified Van der Pol equation. Moreover, the parts are coupled unidirectionally and also the propagation delays are included.
Results: The ECG is computed by adding a trial and ventricular potential differences.
Conclusion: The resultant action potentials and also ECG signal are compared with real data. The results verify the proposed approach.

**Corresponding author: Email: Nikravsh@aut.ac.ir;*

Keywords: Modeling; heart electrical conduction system; Van der Pol equation; ECG; action potential.

ABBREVIATIONS

AM: Atrial Muscles
AP: Action Potential
AV: AtrioVentricular
CB: Common Bundle
DPF: Distal Purkinje Fibers and ventricular muscles
ECG: ElectroCardioGram
CEA: Cardiac Electrical Activity
HECS: Heart Electrical Conduction System
HRV: Heart Rate Variability
mV: miliVolts
PPF: Proximal Purkinje Fibers and ventricular muscles
SA: SinoAtrial
s: seconds
VdP: Van der Pol
V: Volts

1. INTRODUCTION

There are a large number of oscillating cells in the heart which generate heartbeat. A considerable amount of research on the CEA (cardiac electrical activity) modeling has been conducted in the literature [1-10]. The mathematical modeling of the CEA has received considerable attention in recent years. Because of similarity between cardiac AP (Action Potential) and classic VdP (Van der Pol) oscillator behavior [5], this oscillator is considered as a point of entry into the CEA modeling. In one of the oldest papers of Van Der Pol and Van Der Mark, HECS (Heart Electrical Conduction System) has been considered as the coupled VdP oscillators [7]. However, the ECG has not been generated. In [11], Hodgkin and Huxley proposed a mathematical model to describe AP which is applicable to cardiac AP. Recently, [8] has modeled important aspects of the cardiac AP by implementing a modification in classic VdP oscillators. The general aspects of the heart rhythms was demonstrated in [6] by utilizing two coupled VdP oscillators with unidirectional and bidirectional coupling functions. Nevertheless, ECG could not be generated. Some different methods of coupling the oscillators have been studied in [9]. Moreover, [9] has considered time delays between the oscillators. In [3], a mathematical model of the CEA has been proposed by employing three oscillators. The oscillators were indicators of the SA (SinoAtrial) node, the AV (AtrioVentricular) node and the Purkinje fibers. Considering the delays of electrical signal propagation in the heart, its dynamic was represented as a set of delayed differential equations. To solve these equations numerically, the second order Taylor approximation has been employed. In addition, it has been shown that sum of these three oscillators' outputs are similar to the normal ECG. Different ECG signals which demonstrate ventricular flutter, ventricular fibrillation and sinus bradycardia were reconstructed by omitting some coupling coefficients of the oscillators. However, the real ECG signal is the potential difference between the right hand and the left foot which can be interpreted as difference in electrical potential between the SA node and the DPF (Distal Purkinje Fibers and ventricular muscles). As it has been mentioned, although [3] generated the ECG signal, it is not based on the CEA.

The aim of this paper is to generate the ECG signal based on the heart mechanism. To this aim, cardiac cells are divided into six parts namely, the SA node, the AM (Atrial Muscles), the AV node, CB (Common Bundle), the PPF (Proximal Purkinje Fibers and ventricular muscles), and the DPF parts. For each part, VdP oscillator is modified to generate its particular AP. The main contributions of the paper are as follows: first, the ventricular AP is modeled by considering its plateau phase. The plateau phase of ventricular AP has been discussed in more detail in physiological references, such as [12]. Furthermore, its fast depolarization, owing to fast sodium channels, is modeled. Second, each modeled part will be oscillating with its natural frequency unless it is stimulated by the previous part in accordance with actual mechanism of the heart. Third, the actual electrical signal propagation delays of the heart are considered. Finally, the ECG signal is generated by subtracting APs of the heart cells parts.

2. MATERIALS AND METHODS

This section highlights the essential points of CEA which will be considered in the proposed mathematical model. Moreover, some available mathematical models in the literature are modified to correspond more precisely to actual APs in the different heart parts.

2.1 Heart Physiology

There are two kinds of APs in the heart (Fig. 1), namely nodal AP, and non-nodal AP. nodal APs occur in SA and AV nodes and non-nodal ones occur in atrial and ventricular muscles and also Purkinje fibers.

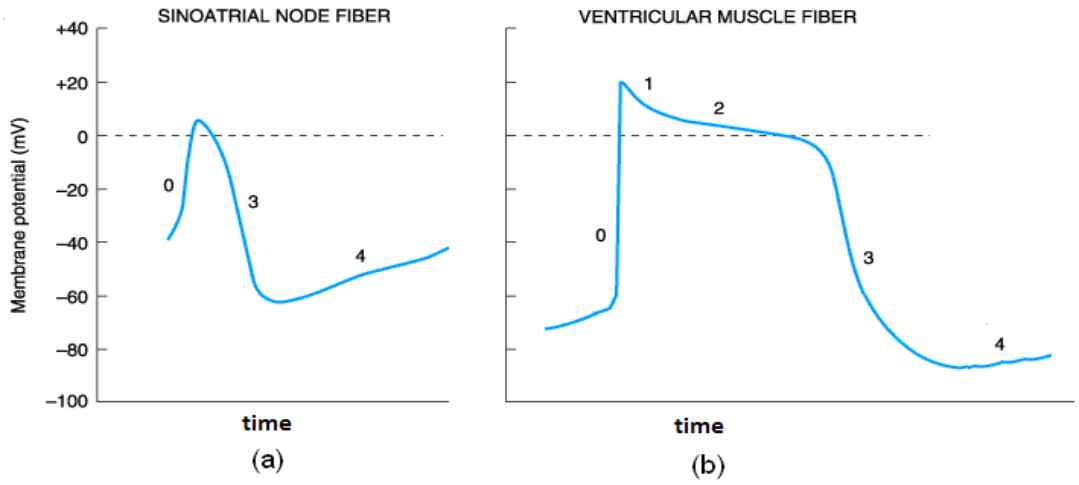

Fig. 1. The graphs of (a) nodal and (b) non-nodal APs [13,15]

The so-called ECG signal is indeed the potential difference between the right hand and the left foot of a person. This potential difference is the resultant of the heart cells' APs. The ECG signal includes P wave that represents atrial depolarization, QRS complex that indicates ventricular depolarization and T wave which manifests repolarization of ventricles.

Each part of the HECS is able to generate electrical impulses and transmit depolarization wave to the other parts. However, each part has different pulse generation rate. Table 1 shows natural frequency ranges of HECS different parts.

Table 1. Natural frequency of the different parts of HECS (CPM (Cycle Per Minute)) [14]

HECS part	Natural frequency (CPM)
SA Node	60-100
AV Node	60-80
Bundle Of His	40-60
Purkinje Fiber	20-40

Assuming SA impulse is generated at t=0, Fig. 2 specifies the time when electrical signals reach to different parts of the heart.

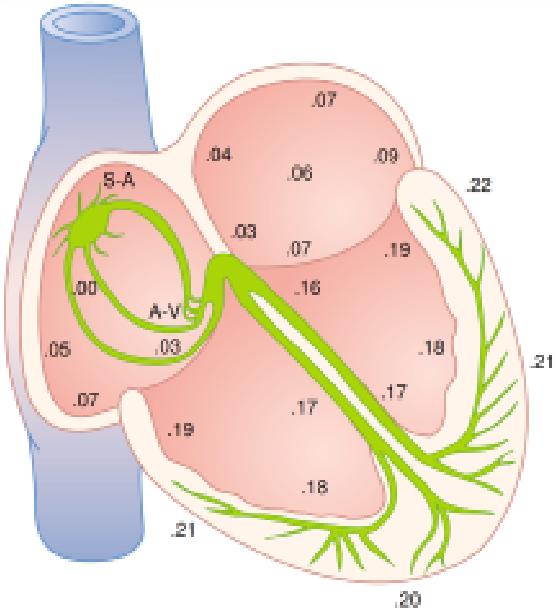

Fig. 2. Signal arrival time in different parts of the heart [12]

2.2 CEA Modeling

Ref [8] argues that using VdP oscillator is a suitable approach to model the heart AP because of the following reasons: first, in the heart the SA node has the highest oscillation frequency and other oscillators are supposed to follow this frequency without any variation in amplitude. Likewise, when VdP oscillator is excited by an external signal with higher frequency, it changes its frequency to the higher one without any variation in amplitude. Second, it is shown that modified VdP oscillator is the simplified Hodgkin-Huxley model which is used to simulate AP [8]. Equation (1) describes dynamics of VdP oscillator:

$$\ddot{x}(t) + \alpha(x^2(t) - \mu)\dot{x}(t) + \omega^2 x(t) = 0 \quad (1)$$

Where $x(t)$ represents the voltage variable, $\omega,\ \mu,$ and α represent limit cycle frequency, limit cycle center, and damping ratio, respectively. Modified VdP oscillator equation, which has been used in the SA and the AV nodes, is as follows [8]:

$$\ddot{x}(t)+\alpha(x(t)-v_1)(x(t)-v_2)\dot{x}(t)+fx(t)(x(t)+d)(x(t)+e)=0 \tag{2}$$

Where $d,\ e,\ -v_1v_2,$ and α should be positive and the inequality $-v_1v_2<d<e$ should be satisfied to have a stable limit cycle. $x(t)$ represents voltage variable, $\dot{x}(t)$ implies current variable, α is the damping ratio, and finally f shows oscillation frequency of coupled oscillators. Equation (2) has three equilibrium points, namely $-e$, $-d$, and the origin. Origin, $-d$, and $-e$ are the unstable focus, the saddle point, and the stable node, respectively. For more information please refer to [8].

Equations (3), (4), (7), and (8) are used to model APs of the six considered parts. These equations have the structure of VdP equation except that some parts have been added to them and also variable change has been applied in order to equalize the amplitude of the equation and the heart AP. Equation (3) is used to model SA and AV action potentials:

$$\begin{aligned}\dot{x}_1(t)&=x_2(t)\\ \dot{x}_2(t)&=-\alpha(x_1(t)-v_1)(x_1(t)-v_2)x_2(t)-fx_1(t)(x_1(t)+d)(x_1(t)+e).\end{aligned} \tag{3}$$

To make AP lie between -65 mV (milliVolts) and +5 mV, equation (3) is rewritten as follows:

$$\begin{aligned}\dot{\overline{x}}_1&=\overline{x}_2\\ \dot{\overline{x}}_2&=-\alpha((\frac{\overline{x}_1-b}{m})-v_1)((\frac{\overline{x}_1-b}{m})-v_2)\overline{x}_2-fm(\frac{\overline{x}_1-b}{m})((\frac{\overline{x}_1-b}{m})+d)((\frac{\overline{x}_1-b}{m})+e)\end{aligned} \tag{4}$$

Where $\overline{x}_1(t)$, $\overline{x}_2(t)$, m, and b are as follows:

$$\begin{aligned}&\overline{x}_1=mx_1+b,\quad \overline{x}_2=mx_2\\ &m=\frac{0.07}{\max(x_1(t))-\min(x_1(t))},\quad b=0.005-m\times\max(x_1(t))\end{aligned} \tag{5}$$

Where $\max(x_1(t))$ and $\min(x_1(t))$ are derived numerically from (3) utilizing Mathematica. Now, based on the previous equations, equation (6) is proposed for the SA and AV nodes:

$$\begin{aligned}\dot{\overline{x}}_1&=\overline{x}_2+\text{coupling}\\ \dot{\overline{x}}_2&=-\alpha((\frac{\overline{x}_1-b}{m})-v_1)((\frac{\overline{x}_1-b}{m})-v_2)\overline{x}_2-fm(\frac{\overline{x}_1-b}{m})((\frac{\overline{x}_1-b}{m})+d)((\frac{\overline{x}_1-b}{m})+e)\end{aligned} \tag{6}$$

Where SA node's coupling term is zero and AV node one is as follows:

$$\text{coupling} = k_{AM-AV}(\overline{x}_{1_{AM}}(t - \tau_{AM-AV}) - 1.2\overline{x}_{1_{AV}}(t)).$$

$\overline{x}_{1_{AM}}$ is AM's action potential. Since ions flow from higher voltage to lower voltage, the coupling term is dependent on voltage difference between two cardiac parts [3]. Furthermore, k_{AM-AV} determines coupling coefficient. As a result, we add the coupling term to $\overline{x}_2(t)$ in this paper.

The following equation is proposed for the AM, CB, the PPF and the DPF action potential:

$$\begin{aligned}\dot{x}_1 &= x_2 \\ \dot{x}_2 &= -\alpha(x_1 - v_1)(x_1 - v_2)(x_2 + hx_2^{\,2}) - fx_1(\gamma - \beta\cos(x_1)).\end{aligned} \tag{7}$$

As it can be deduced from equations (1) and (2), rising and falling slopes of VdP and the modified VdP equations are equal, while it is not applicable to APs of some parts of the heart. To address this problem, the term $hx_2^{\,2}(t)$ is added. Furthermore, $\gamma - \beta\cos(x_1(t))$ causes ventricular fiber AP to produce a peak (see Fig. 1.b, region 1). These modifications cause better concordance between actual heart AP and our mathematical model. To make AP lie between -80 mV and +20 mV, the equation (7) is rewritten as follows:

$$\begin{aligned}\dot{\overline{x}}_1 &= \overline{x}_2 + \text{coupling} \\ \dot{\overline{x}}_2 &= -\alpha((\frac{\overline{x}_1 - b}{m}) - v_1)((\frac{\overline{x}_1 - b}{m}) - v_2)(\overline{x}_2 + \frac{h}{m}\overline{x}_2^{\,2}) - fm(\frac{\overline{x}_1 - b}{m})(\gamma - \beta\cos(\frac{\overline{x}_1 - b}{m}))\end{aligned} \tag{8}$$

Where $\overline{x}_1(t),\ \overline{x}_2(t),\ m,$ and b are defined as follows:

$$\begin{aligned}&\overline{x}_1 = mx_1 + b, \quad \overline{x}_2 = mx_2 \\ &m = \frac{0.1}{\max(x_1(t)) - \min(x_1(t))}, \quad b = 0.02 - m \times \max(x_1(t)).\end{aligned} \tag{9}$$

Numerical solution of equation (7) yields $\max(x_1(t))$ and $\min(x_1(t))$ which are used in equation (9). Coupling term in equation (8) is used to demonstrate the effect of one part on the next part. The Coupling terms of AM, CB, PPF, and DPF parts are described in the following equations:

$$\begin{aligned}\text{coupling}_{AM} &= k_{SA-AM}(1.2\overline{x}_{1_{SA}}(t - \tau_{SA-AM}) - \overline{x}_{1_{AM}}(t)) \\ \text{coupling}_{CB} &= k_{AV-CB}(1.2\overline{x}_{1_{AV}}(t - \tau_{AV-CB}) - \overline{x}_{1_{CB}}(t)) \\ \text{coupling}_{PPF} &= k_{CB-PPF}(\overline{x}_{1_{CB}}(t - \tau_{CB-PPF}) - \overline{x}_{1_{PPF}}(t))\end{aligned}$$

$$\text{coupling}_{DPF} = k_{PPF-DPF}(\overline{x}_{1_{PPF}}(t - \tau_{PPF-DPF}) - \overline{x}_{1_{DPF}}(t)).$$

The actual ECG signal is the potential difference between the right hand and the left foot which can be interpreted as the proximal and distal heart potential difference. Since there exists an insulating connective tissue between the atria and the ventricles, we supposed two AP differences instead of using one AP difference between the proximal and distal heart. The first part is the potential difference between the proximal and distal atria (the SA and AV nodes), and the second part is the potential difference between the proximal and distal ventricles (the CB and the DPF parts). To build ECG signal, these two AP differences are added together (equation (10)). A weighting constant has been used to weight two terms according to their effect on ECG signal. Since the R wave in ECG is associated with ventricles and the P wave is pertain to atria which its amplitude approximately 0.2 of R wave amplitude, weighting constant is set to 0.2.

$$ECG = 0.2(x_{1_{SA}} - x_{1_{AV}}) + (x_{1_{CB}} - x_{1_{DPF}}). \tag{10}$$

3. RESULTS AND DISCUSSION

The proposed approach is evaluated by a variety of simulations. Numerical parameters are described in Tables 2, 3, and 4. The parameters have been computed numerically using the equations achieved in subsection 2.2 by Mathematica software. In addition, MATLAB software is used to construct the cardiac electrical signals. Dormand-Prince (PKDP) numerical method has been utilized to solve AP equations.

Table 2. Numerical parameters of the SA and the AV nodes

	α	v_1	v_2	f	d	e	$\max(x_1(t))$	$\min(x_1(t))$
SA node	6.7	2	-2	5.34	5	19	3.37	-4.65
AV node	5	2	-2	3	5	19	3.38	-4.65

Table 3. Numerical parameters of AM, CB, PPF, and DPF parts

	α	v_1	v_2	f	h	γ	β	$\max(x_1(t))$	$\min(x_1(t))$
AM	3.5	6	-2	213	0	2	1.8	9.59	-6.42
CB	5	5	-2.6	435	0.0031	2	1.98	8.9	-6.35
PPF	3.8	5	-2.3	302	0.0025	2	1.99	8.67	-6.31
DPF	3	5.4	-2.2	220	0.002	2	1.99	9.07	-6.47

Table 4. Numerical parameters of coupling terms

	SA-AM	**AM-AV**	**AV-CB**	**CB-PPF**	**PPF-DPF**
k	0.5	0.5	0.5	0.5	0.5
$\tau(s)$	0.0567	0.49	0.1333	0.6098	0.5682

Fig. 3 represents the voltage wave of considered parts when there is no coupling between them. As it can be seen in this figure, each part has its unique oscillation frequency.

Table 5 represents natural frequency of six parts in the case that they have not been stimulated by previous adjacent parts. As it can be seen, the SA natural frequency is more than the other parts. As long as the SA node functions normally, the other parts oscillate by SA frequency. But if SA signal does not reach to other parts, they will oscillate by AM natural frequency which is more than the others.

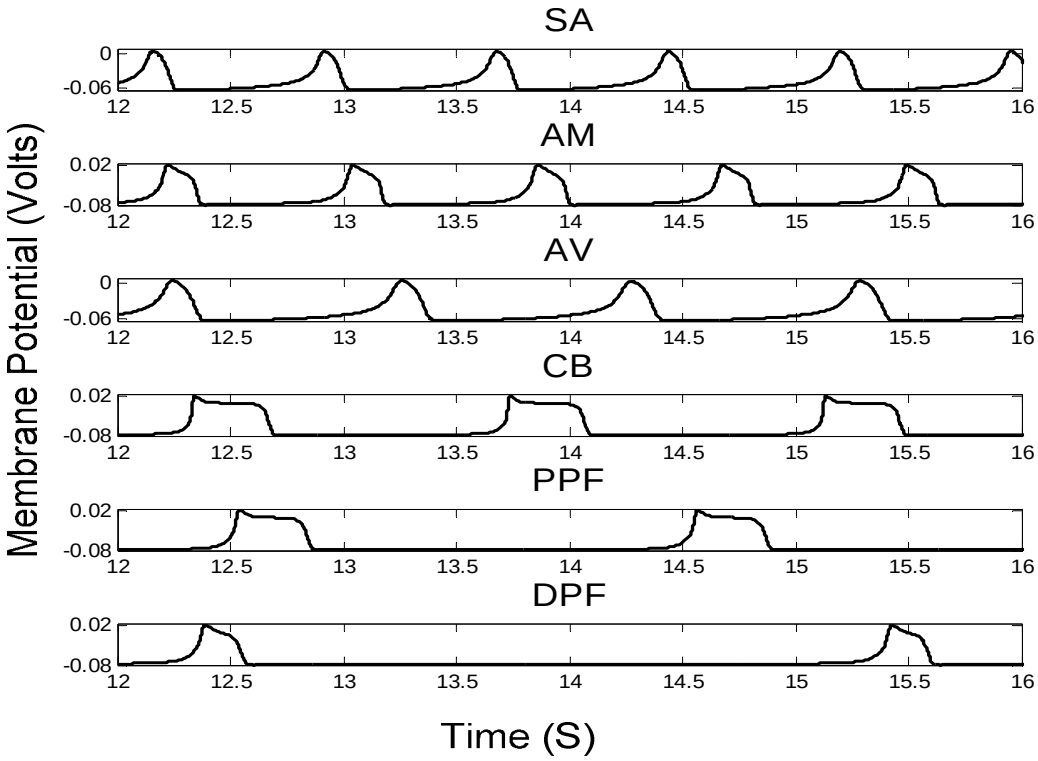

Fig. 3. Six parts' AP ignoring coupling effect among them

Table 5. Natural frequencies of the six considered heart parts

	SA	AM	AV	CB	PPF	DPF
Cycles Per Minute	80	75	60	40	33.33	20
Period	0.75s	0.9375s	1s	1.5s	2s	3s

From Figs. 4 upto 10, coupling terms among six parts of the heart have been considered. Fig. 4(a) represents APs of the six parts. As it can be seen, APs of the SA and the AV nodes do not have plateau phase and are slow in depolarization phase. However, the other parts have a fast depolarization phase and contain plateau phase which have been considered in the paper unlike the preceding researches in the literature [3-4]. The applied delays among six parts of the heart are in accordance with Fig. 2. Fig. 4(a) is magnified in Fig. 4(b) to show the time delays more obviously.

Table 6 represents quantitative details of different phases of heart's six-part APs. Real data which has been adopted from [12-15], is about an adult, healthy man in relaxed condition. This table represents the ratio of refractory period to cardiac cycle. Moreover, it represents

the quantitative details of threshold, resting, and positive peak of APs of the six parts. As it can be seen in the Table 6, the simulation results are akin to real ones.

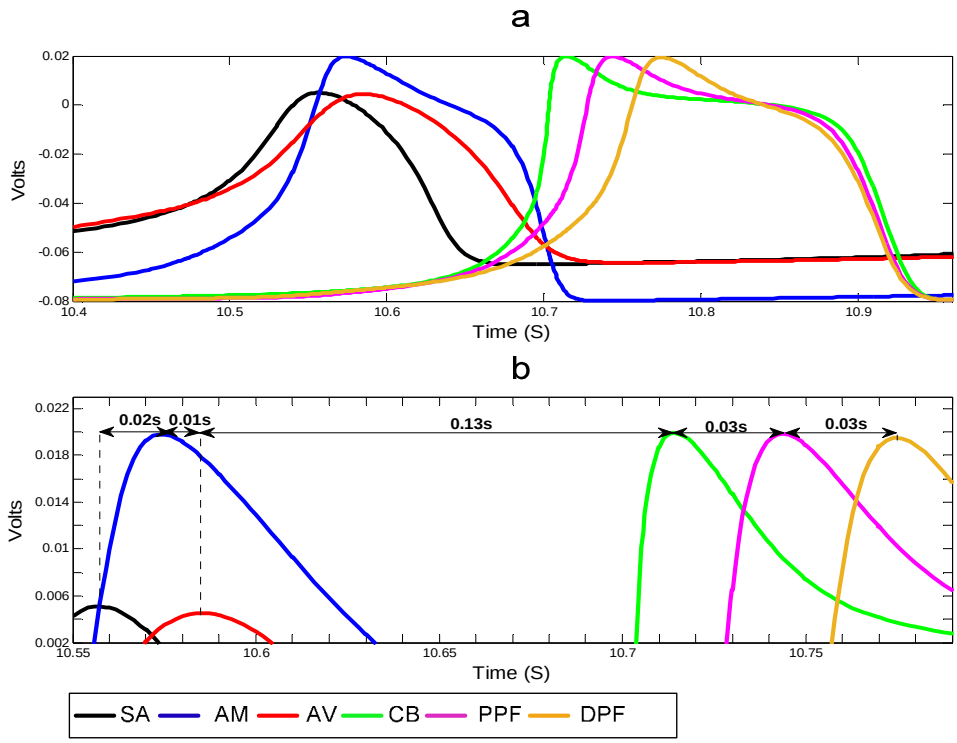

Fig. 4. (a) APs of six different parts of the heart. (b) The magnified version of (a) to show the time delays between two adjacent parts more obviously

Table 6. Quantitative details of six-part APs

Parts	Ratio of refractory period to cardiac cycle (%)		Threshold potential (mV)		Resting potential (mV)		Positive peak potential (mV)	
	Real	Simulated	Real	Simulated	Real	Simulated	Real	Simulated
SA	25	27	-45	-45	-65	-65	10	5
AM	27	31	-57	-60	-80	-80	15	20
AV	26	32	-45	-45	-65	-65	10	5
CB	37	34	-60	-60	-80	-80	20	20
PPF	33	31	-60	-60	-89	-80	20	20
DPF	28	29	-60	-60	-89	-80	20	20

In Fig. 5, AP of each cardiac part is mapped to its position in the heart.

It is worth mentioning that in ventricles, the cell which is depolarized at first is repolarized at last which results in a positive T wave. This point has been considered in the simulation and is represented in Fig. 6. The ventricular tissue has been divided into three parts where depolarization electrical signal is initialized in CB, and then it reaches to PPF. In the next step, it arrives to the DPF. Completely different from depolarization phase, repolarization phase is initiated in the DPF and is terminated in CB.

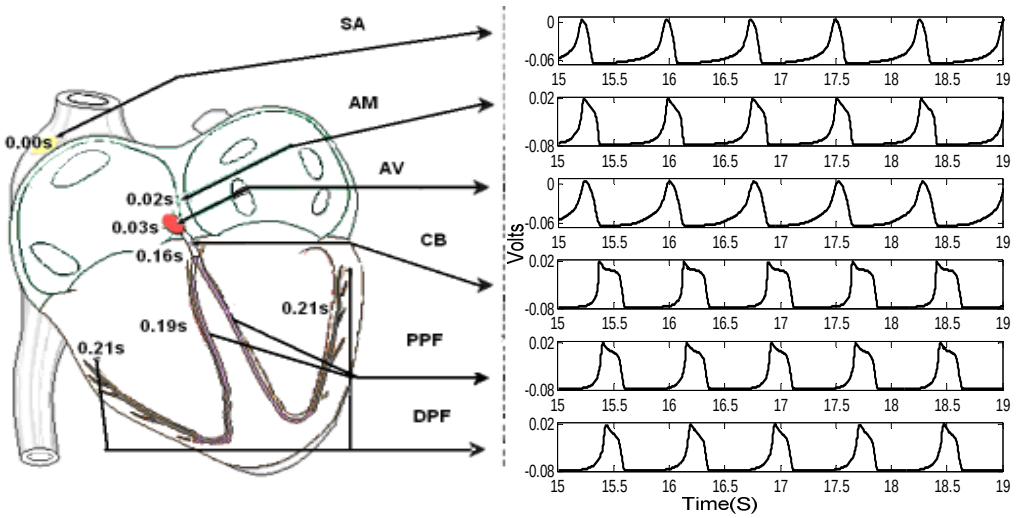

Fig. 5. APs of different parts with mapping onto their positions in the heart

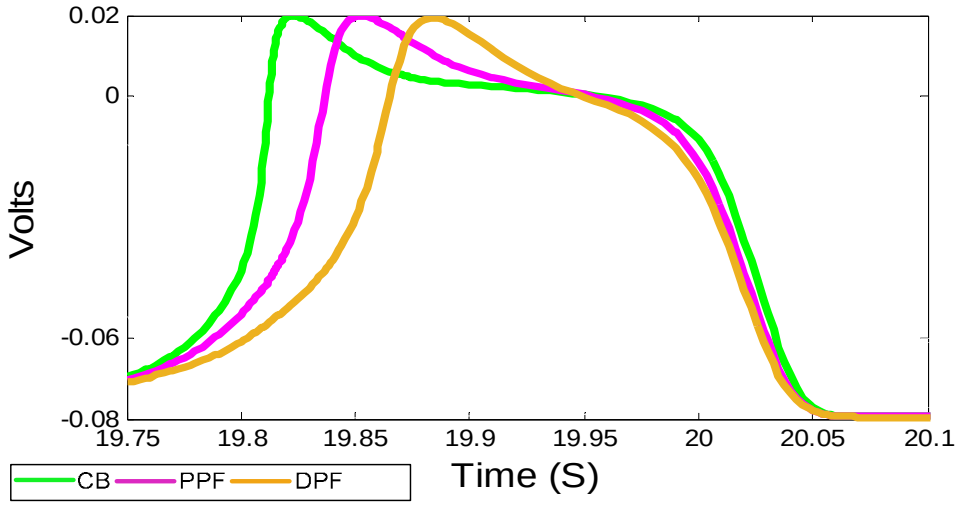

Fig. 6. Ventricular AP graph

In Fig. 7, the achieved phase planes of AP in six considered parts have been depicted. Variable x_2 represents the rate of APs. Absolute value of x_2 is small in SA and AV phase planes. Therefore APs of the SA and AV nodes fall and rise slowly. Variable x_2 has larger positive amplitude in AM and ventricular parts (CB, PPF, and DPF). Hence, increasing rates of these four parts are remarkable. Moreover, the SA's phase plane is akin to AV's one. The APs of AM and ventricular parts have plateau phase and phase planes of these parts are similar. The mentioned points of Fig. 7 are in accordance with reality.

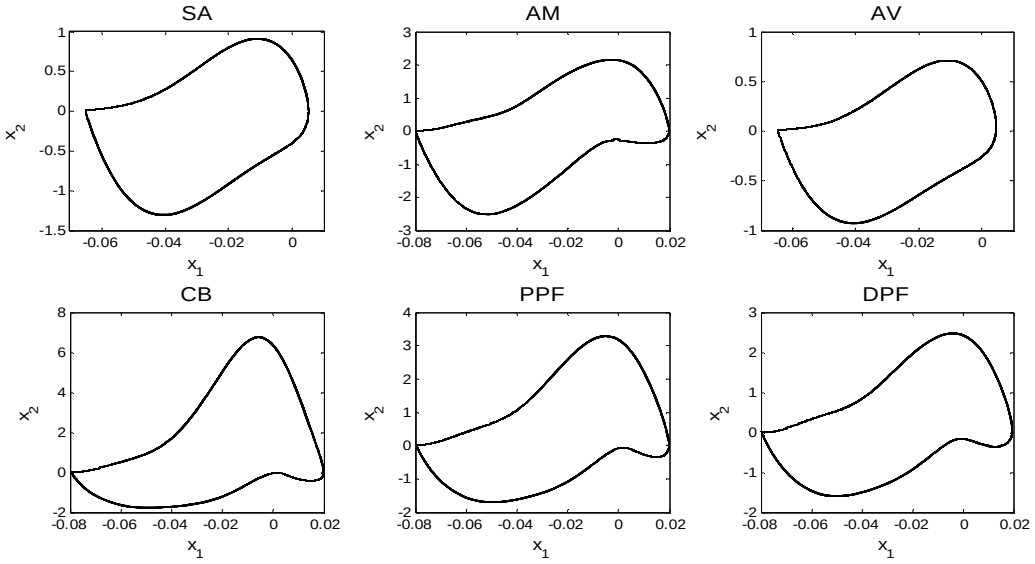

Fig. 7. Phase planes of the model based APs

Two ECG signals are represented in Fig. 8. The upper one and the lower one are obtained from actual data and mentioned model, respectively. As it can be seen in this figure, signals are almost similar to each other. Moreover, model based ECG has P, Q, R, S and T waves with reasonable time intervals. Actual data of Figs. 8, 9, and 10 is obtained from [16].

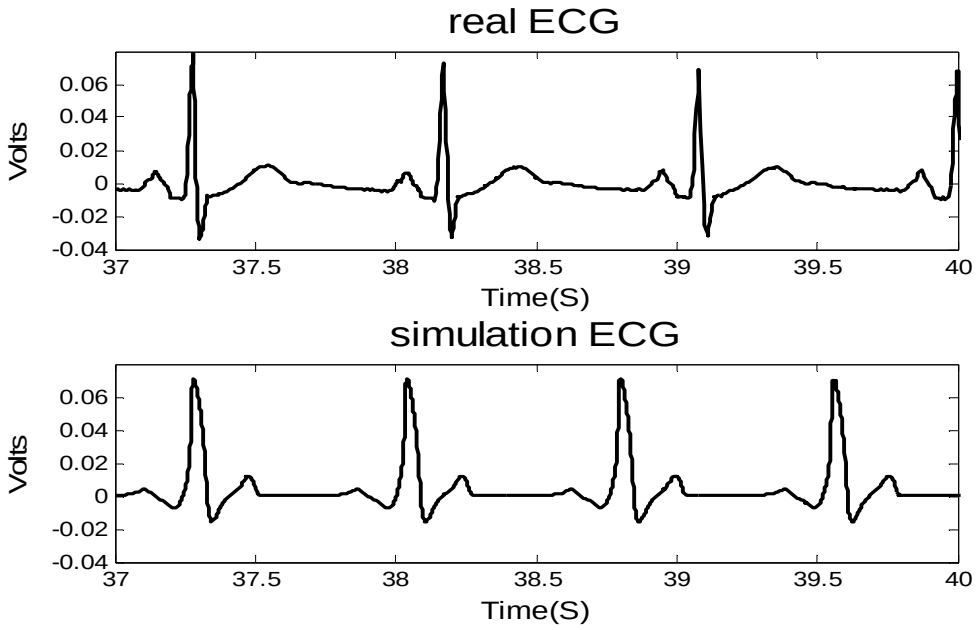

Fig. 8. Time curve of ECG based on real data and the mathematical model

Fig. 9 depicts the details of a cardiac cycle. The upper panel is obtained from actual data and the lower one is based on the proposed model. Table 7 expresses numerical values of P, Q, R, S, and T waves of ECG in Fig. 9. Table 8 represents numerical values of segments and intervals in Fig. 9. As it can be seen in these tables, results of the proposed model are almost similar to actual data, except in few cases such as duration of R wave and QRS complex. QRS complex of proposed model appears wider than in actual data because ventricular AP upstroke of the model is slower than actual one.

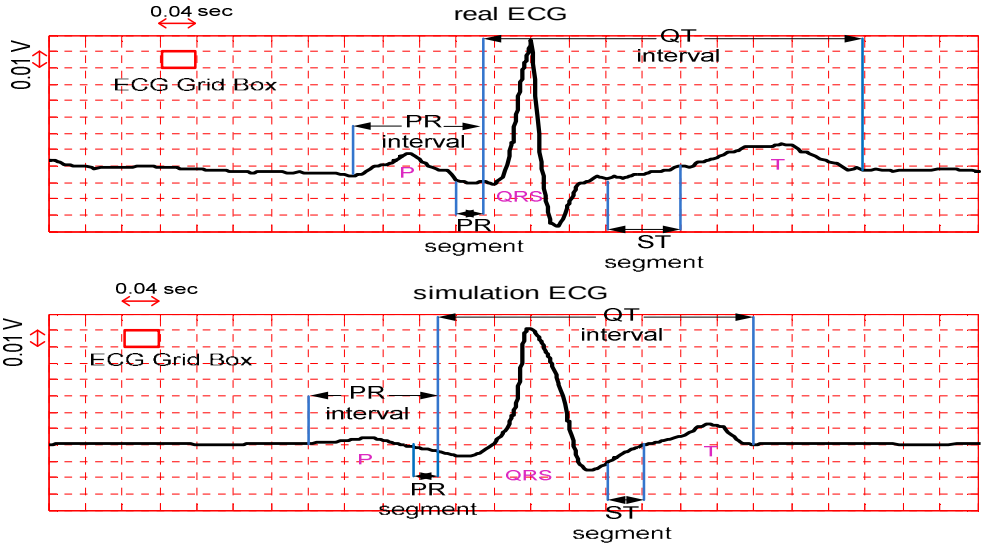

Fig. 9. One cycle of ECG signal based on real data and the mathematical model

Table 7. Quantitative details of P, Q, R, S, and T waves

Waves	Duration (ms)		Amplified Amplitude (mV)	
	Real	Simulated	Real	Simulated
P	90	80	6…8	4
Q	70	80	-8…-11.5	-7.5
R	40	80	60…70	72
S	50	70	-28…-36	-16
T	130	100	11…13	12

Table 8. Quantitative details of intervals and segments in ECG signal

Parts of ECG	Duration (ms)		Ratio to cardiac cycle (%)	
	Real	Simulated	Real	Simulated
PR Segment	30	25	4	3.33
PR Interval	140	140	18.7	18.7
QRS Complex	160	230	21.3	30.7
ST Segment	80	40	10.7	5.3
QT Interval	400	340	53.3	45.3

It is worth mentioning that there is a variation of heartbeat time interval, known as HRV (Heart Rate Variability). HRV is the result of interaction between substantial oscillators with different natural frequencies. However, the proposed model utilizes six oscillators to simulate

the CEA. As a consequence, the resultant HRV has subtle difference with experimental HRV. It leads to a considerable difference in the model based ECG and real one. To meet the challenge, one can employ phase plane approach as shown in Fig. 10. There are some similarities between real data based phase plane and model based one. Nevertheless, real data based one is torus- like; in contrary to model based one which is a closed path.

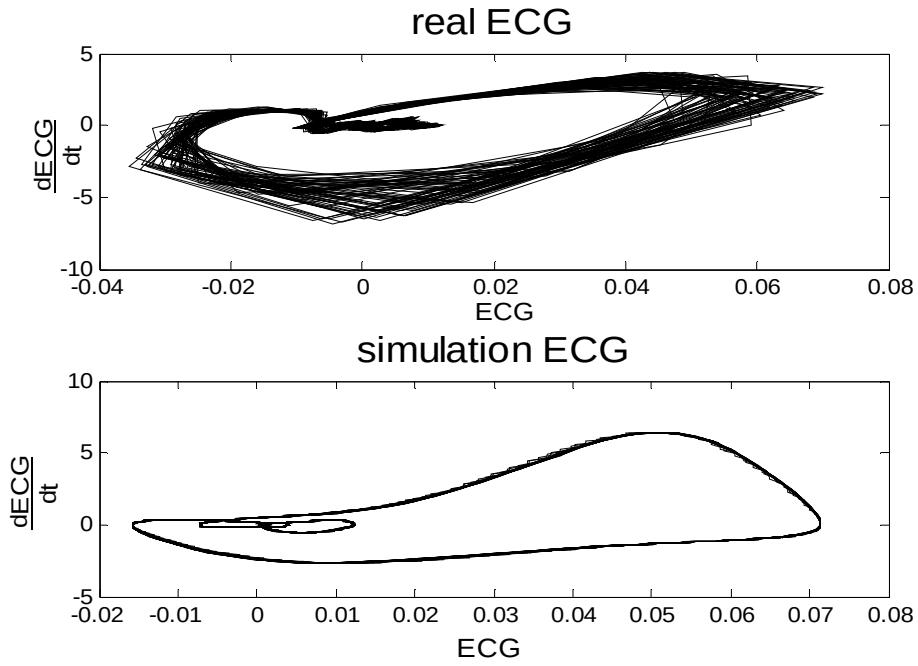

Fig. 10. Comparison of real data based ECG phase plane and model based one

In comparison with the previous researches, the main novelty of the paper are as follows: two kinds of APs which exist in heart, namely slow response AP and fast response AP, have been modeled in the paper to generate ECG signal. While in the previous researches, just slow response AP has been employed to model ECG. Moreover, the fast response AP is constructed by considering its plateau phase. Furthermore, each modeled part will be oscillating with its natural frequency unless it is stimulated by the previous part in accordance with actual mechanism of the heart. Also, the cardiac coupling is modeled as a function of potential difference between two adjacent cardiac parts. It should be noted that in ventricles, the cell which is depolarized at first, is repolarized at last which results in a positive T wave. This fact has been considered in the paper to generate ECG. Finally, the ECG signal is built up by subtracting APs of the cardiac parts.

4. CONCLUSION

The main goal of this paper was to model the CEA based on the heart physiology and this model was used to generate ECG signal as well. To this aim, the cardiac cells were divided into six parts. For each part, VdP oscillator was modified to generate its particular AP. The resultant ECG was achieved by adding atrial and ventricular potential differences. The computed AP of each part and the simulated ECG signal were compared with actual data. There are some opportunities to extend the scope of the study. For instance, it is recommended to ponder over HRV. Furthermore, in the heart, there are three paths between

the SA and AV nodes. However, the paper considered just one of them. As a result, one can divide cardiac cells into more parts to achieve a better modeling of the CEA.

COMPETING INTERESTS

Authors have declared that no competing interests exist.

REFERENCES

1. Holland NL. The dynamics of coupled oscillator. MS thesis. Wellington: Victoria University; 2008.
2. Sheheitli H, Rand R. Origin of arrhythmias in a heart model. Commun Nonlinear Sci Numer Simulat. 2009;14:3707-3714.
3. Gois SRFSM, Savi MA. An analysis of heart rhythm dynamics using a three-coupled oscillator model. Chaos, Solitons and Fractals. 2009;41:2553-2565.
4. Rompala et al. Dynamics of three coupled Van der Pol oscillators with application to circadian rhythms. Communications in Nonlinear Science and Numerical Simulation. 2007;12:794-803.
5. Van Der Pol B. On relaxation oscillation. Philosophical Magazine. 1926;2(11):978-992.
6. Santos AM, Lopes SR, Viana RL. Rhythm synchronization and chaotic modulation of coupled Van der Pol oscillators in a model for the heartbeat. Physica A. 2004;338:335-355.
7. Van Der Pol B, Van Der Mark J. The heartbeat considered as a relaxation oscillator and an electrical model of the heart. Philosophical Magazine. 1928;6:763-775.
8. Grudzinski K, Zebrowski JJ. Modeling cardiac pacemakers with relaxation oscillators. Physica A. 2004;336:153-162.
9. Cambel SR, Wang D. Relaxation oscillators with time delay coupling. Physica D. 1998;111:151-178.
10. Suchorsky M, Rand R. Three Oscillator of the heartbeat generator. Commun Nonlinear Sci Numer Simulat. 2009;14:2434-2449.
11. Hodgkin AL, Huxley AF. A quantitative description of membrane current and its application to conduction and excitation in nerve. J Physiol. 1952;117:500-544.
12. Guyton AC, Hall JE. Textbook of medical physiology. 9th ed. Philadelphia: W.B. Saunders Company; 1996.
13. Plonsey R, Barr RC. Bioelectricity A Quantitative Approach. 3rd ed. New York: Springer Science and Business Media; 2007.
14. Katz AM. Physiology of the Heart. 3rd ed. Philadelphia: Lippincott, Williams, and Wilkins; 2001.
15. Gharooni M, Gharooni A, Gharooni H, Ebrahimi P, Nazoori S, Amin M, Hemmatyar N. Atlas of Electrocardiography GHAROONI. 7th ed. Tehran: Arjomand Publication, 2012. Persion.
16. Penzel T, Moody GB, Mark RG, Goldberger AL, Peter JH. The Apnea-ECG Database. Computers in Cardiology. 2000;27:255-258. Accessed 21 September 2013. Available: http://physionet.org/physiobank/database/apnea-ecg/

Peer-review history:
The peer review history for this paper can be accessed here:
http://www.sciencedomain.org/review-history.php?iid=582&id=32&aid=5630